

## Nucleation and growth of $\mu$ phase

K. ZHAO, L. H. LOU, Y. WEN, H. LI, Z. Q. HU

*Institute of Metal Research, Academia Sinica, Shenyang 110015, People's Republic of China*

*E-mail: kzhao@imr.ac.cn*

The  $\mu$  phase is a topologically-closed-packed phase in the superalloys containing a high content of Mo and W, and belongs to a rhombohedral lattice with parameters  $a = 0.476$  nm,  $c = 2.56$  nm in a hexagonal system [1]. Its presence in a  $\gamma$  matrix has been found to be detrimental to some properties of alloy such as rupture strength, room temperature tensile ductility, impact toughness and corrosion resistance [2, 3]. On the other hand it was also shown that moderate amounts of platelet-like  $\mu$  phase particles did not affect the tensile properties and the impact strength at room temperature [4]. The properties may be affected by the precipitation of  $\mu$  phase via several mechanisms [3]. The first is due to the intrinsic brittleness of the  $\mu$  phase. The hard  $\mu$  phase acts as a barrier to moving dislocations which pile-up at the interface, leading to interfacial decohesion and crack initiation. The second is that many refractory elements, acting as important solid-solution strengtheners in superalloys, are scavenged from the  $\gamma$  matrix and concentrated in the  $\mu$  phase. Therefore, precipitation of the  $\mu$  phase is mostly unfavorable in service.

The purpose of this study is to make clear how  $\mu$  phase nucleates and grows. Then, measures will be proposed to prevent its formation.

The nominal chemical composition (wt%) of the experimental nickel-base was superalloy mainly consisting of 16Cr, 8W, 1.5Mo, 5Al, Nb + Co < 5% and Ni bal. The alloy was directionally solidified by HRS process in an industrial vacuum induction furnace. The withdrawal rate was 7 mm/min. The thermal gradient was approximately 50 °C/cm at the solidifying interface. The mold was heated by two heat sources, so that the upper temperature was 1500 °C and the lower one 1550 °C. The size of cylindrical specimens was  $\phi 16 \times 170$  mm. The directionally solidified specimens were isothermally aged at 900 °C for 500 h without solution heat treatment. All of specimens were etched by 210 ml  $H_3PO_4$  + 170 ml  $H_2SO_4$  + 120 ml  $H_2O$ . As a result, the  $\gamma$  matrix showed black in optical microscope or scanning electron microscope, while the  $\gamma'$  and  $\mu$  phases white and bright. Cross-sectional specimens were then observed by using SEM.

Primary  $\mu$  phase was not observed in the as-cast specimens. The shape of the  $\gamma'$  phase was cubic with a mean size of 0.3  $\mu$ m (Fig. 1) at the interdendritic area. The volume fraction of  $\gamma'$  phase was very high in this alloy. As shown in Fig. 2, however, a large amount of  $\mu$  phase precipitated in specimens aged for 500 h. These  $\mu$  phase particles observed were mainly located at interdendritic area. The  $\mu$  phase was not homogeneously distributed but rather concentrated which can

be explained as the result of microsegregation [5]. The concentration of solutes was rather different at interdendritic area and dendrite core. Mo and W, the major constituents of the  $\mu$  phase, had different segregation behaviors. Mo was a positive segregation element, and W negative. So Mo was rather concentrated at interdendritic area, and W at dendrite core. Therefore, Cai and Zheng [5] concluded Mo had higher tendency to form a  $\mu$  phase than W. However, the content of Mo was low in this experimental alloy.

Forming  $\mu$  phase needs two stages: nucleation and growth. Li and Liu [6] pointed out that the  $\mu$  phase has almost the same crystal structure and compositions as  $M_6C$ . As we know, nucleation is almost always heterogeneous. The free particle surface increases the free energy of the material. Thus, nucleation on the free particle surface results in decrease of some free energy. If the structures are similar, surface energy can be decreased more during nucleation. Therefore, in order to nucleate effectively,  $M_6C$  fine particles will act as nucleation sites of  $\mu$  phase, which can be clearly seen in Fig. 3, where the white  $M_6C$  particle has clearly provided a nucleation site for  $\mu$  phase.

It is well known that C, a strong positive segregation element, distributes mainly at interdendritic area. Accordingly, carbide particles, including  $M_6C$ , distribute here. Nucleation of  $\mu$  phase then occurs on  $M_6C$  particles. This was also reported by Sims *et al.* [7]. Consequently, it is due to the microsegregation of C, Mo and W.

Microstructures in Fig. 3 also illustrate another point that the  $\mu$  phase grows principally from the  $\gamma'$  phase instead of the  $\gamma$  matrix. This is not consistent with other papers.

Simonetti [4] pointed out that  $\mu$  phase particles precipitated from the  $\gamma$  matrix which was in turn depleted in elements such as W, Mo, Cr and which transformed into  $\gamma'$  phase. This led to a microstructure where the  $\mu$  phase particles were surrounded by the  $\gamma'$  phase. However, it is not true here. As shown in Fig. 3, there clearly existed phase boundary between the  $\mu$  phase and the  $\gamma$  matrix, with lack of the so-called  $\gamma'$  phases film around  $\mu$  phase. Although some  $\mu$  phase particles were surrounded somewhere by the  $\gamma'$  phase, these cannot precipitate secondarily due to the size and morphology of  $\gamma'$  phase, which are almost 0.4  $\mu$ m.

The reason perhaps is that forming  $\mu$  phase has consumed many refractory elements of  $\gamma'$  phase. It needs more to grow, so refractory elements from the vicinity  $\gamma'$  phase diffuse to keep continuous grow of  $\mu$  phase at 900 °C, that makes the surrounding  $\gamma'$  phase close to  $\mu$

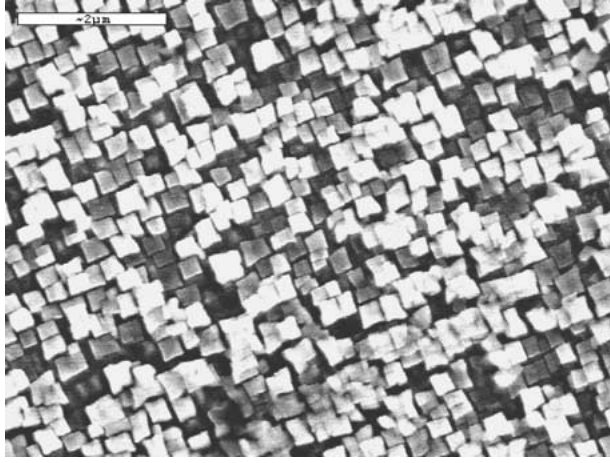


Figure 1 Microstructure of as-cast alloy at interdendrite area.

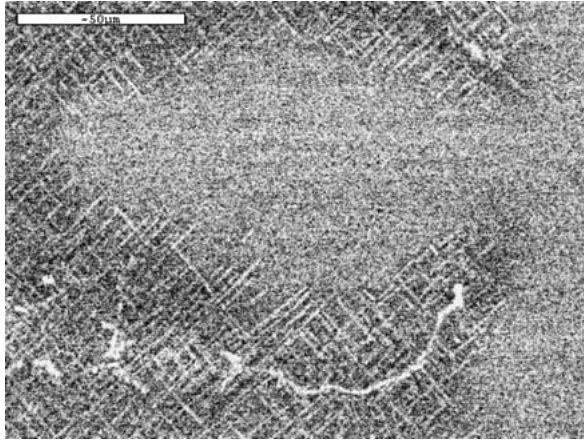


Figure 2 Distribution of  $\mu$  phase.

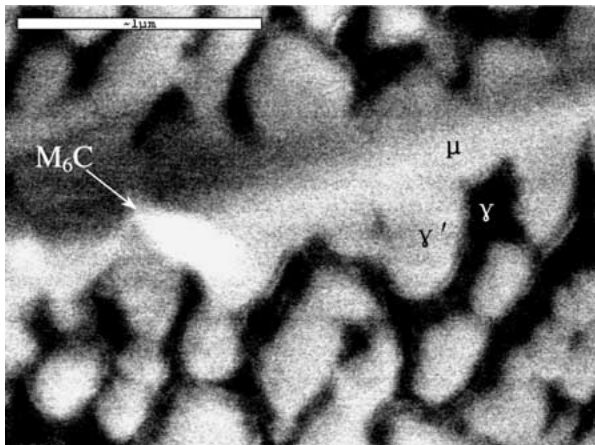


Figure 3 Relation of  $\mu$  phase,  $M_6C$ ,  $\gamma'$ , and  $\gamma$  matrix.

phase. Therefore, the phase boundary between  $\mu$  phase and  $\gamma'$  phase is not clear, as confirmed in Fig. 3.

According to Fig. 4, it can be concluded that the  $\mu$  phase almost precipitates with definite direction. It is well known during directional solidification, competitive growth between the randomly orientated equiaxed grains nucleated at the chill results in the development of a preferred orientation. Since in face-centered-cubic (fcc) structured alloys the dendrites grow along the  $\langle 001 \rangle$  directions, grains with the orientation close to that of the solidification direction will grow predom-

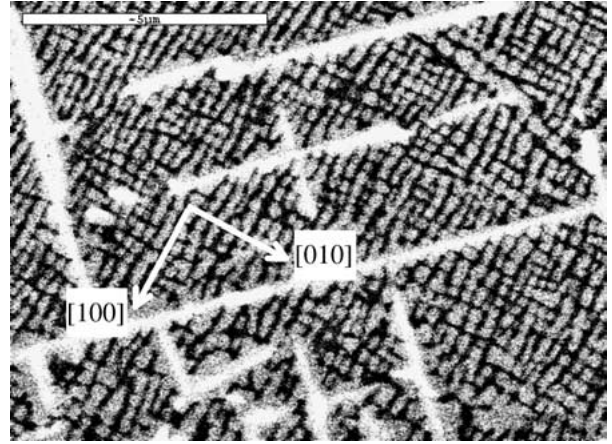


Figure 4 Precipitate faces of  $\mu$  phase along  $\gamma'$  phases.

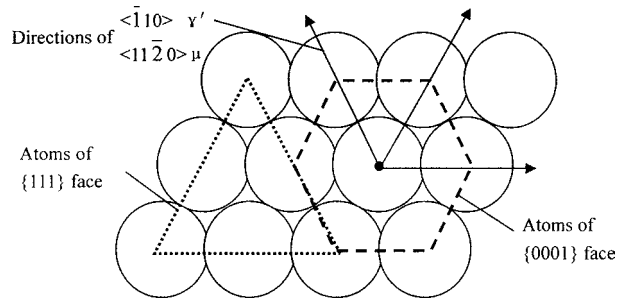


Figure 5 Close-packed face and parallel directions of  $\gamma'$  and  $\mu$  phase.

inately. Then, as shown in the Fig. 4, we can deduce other directions.

The  $\mu$  phase belongs to hexagonal structure and  $\gamma'$  phase fcc crystal structure. As seen from Fig. 5,  $\{0001\}$  face of  $\mu$  phase and  $\{111\}$  face of  $\gamma'$  phase are both hexagonal close-packed. A coherent boundary can be easily formed in their hexagonal close-packed faces.

In order to nucleate, atoms, mainly W, Mo, Cr and so on, in  $\gamma'$  phase diffuse together to form  $\mu$  phase around fine  $M_6C$  particles. Subsequently, these atoms arrange a new crystal structure. During this course, the free energy difference can be expressed as

$$\Delta G = -V\Delta G_v + A\gamma + V\Delta G_s,$$

where  $\Delta G_v$  is the volume energy difference,  $\gamma$  is surface energy, and  $\Delta G_s$  is strain energy for the volume change of new precipitate phase. If the new phase precipitates coherently with the basal plane, it needs the lowest surface energy. Consequently, growth is easy when  $\mu$  phase precipitates from the  $\gamma'$  phase. Therefore, the coherent boundary will be formed between  $\mu$  phase and  $\gamma'$  phase in their close-packed faces, which leads to orientation relationship as  $(111)_{\gamma'} // (0001)_{\mu}$  and  $\langle \bar{1}10 \rangle_{\gamma'} // \langle 11\bar{2}0 \rangle_{\mu}$ .

As the  $\mu$  phase has a hexagonal structure,  $\{0001\}$  face is acted as the basal plane which has the lowest surface energy, and two-dimensional nucleation and growth occur on the edges but not on the basal planes. It comes out that morphology of  $\mu$  phase will be shown as platelet-like.

The following conclusions can be drawn:

1. Owing to microsegregation of some alloying elements,  $\mu$  phase mainly locates at interdendritic area.

The precipitation tendency decreases after solution heat treatment.

2. Nucleation of  $\mu$  phase often occurs on  $M_6C$ . After nucleation,  $\mu$  phase grows mainly on the edges to show platelet-like morphology.

3.  $\mu$  phase precipitate has an orientation relationship with  $\gamma'$  phase as  $(111)_{\gamma'}/(0001)_{\mu}$  and  $\langle\bar{1}10\rangle_{\gamma'}/\langle 11\bar{2}0\rangle_{\mu}$ .

### Acknowledgment

The authors are grateful to Prof. Y. Zhang and Dr. J. Zhang for their assistance in the study and helpful discussion on the results.

### References

1. J. ZHU and H. Q. YE, *Scripta Metall. Mater.* **24** (1990) 1861.
2. H. M. TAWANCY, *J. Mater. Sci.* **31** (1996) 3929.
3. CHESTER T. SIMS and WILLIAM C. HAGEL, "The Superalloys" (John Wiley & Sons, Inc., 1972) p. 264.
4. M. SIMONETTI, *Mater. Sci. Eng.* **A254** (1998) 1.
5. Y. L. CAI and Y. R. ZHENG, *Acta Metall. Sinica.* **1** (1982) 18.
6. Y. Q. LI and J. Y. LIU, "Precipitate Phase of Superalloys in Grain Boundary" (Metallurgy Publishing Company of Technology, Beijing, 1990) p. 30.
7. C. T. SIMS, *et al.*, "Superalloys II" (John Wiley & Sons, 1987) p. 117.

*Received 11 June*

*and accepted 23 June 2003*